UDC 681.5.01 (045)

V. Boiko , V. Apostolyuk

INTEGRATED SYSTEM OF INCIDENCE ANGLE MEASUREMENT

Introduction

Incidence angle is an important concept, as aircraft wings stall when angle of attack gets too large, at a value known as the "critical" incidence. As pilots are taught in flight training, an aircraft can stall at any speed if this critical angle of attack is exceeded. Hence, a great way to avoid stalls is to not let the angle of attack reach critical, and the best way to avoid critical angle of attack is to know value of this angle in the first place.

There are two basic approaches of increasing accuracy of flight parameters measurements. First is to use more accurate sensors and cost of it becomes prohibitively large. An alternative approach, which has received much attention in recent years, is known as integrated systems [1]. This technique employs some additional source of information, external from the given system, to improve the accuracy of the incidence angle measurement system. Careful selection of fundamental characteristics leads to low cost, but potentially very accurate.

In this paper we suggest that the incidence value is obtained from two independent sensors: pitot tube and accelerometer. To reduce measurement errors, the stationary optimal multidimensional filter will synthesized.

Problem formulation

Main goal of this paper is to synthesise optimal stationary stochastic multidimensional filter to combine output signals from pitot tube and accelerometer to produce accurate measurement of an aircraft incidence angle. In order to achieve this task appropriate mathematical models of both sensors must be developed and then combined together using optimal filter, synthesised using Wiener approach.

Pitot tube and accelerometer models

The pitot tube is mounted on the aircraft so that the center tube is always pointed in the direction of travel and the outside holes are perpendicular to the center tube. Since the outside holes are perpendicular to the direction of travel, these tubes are pressurized by the local static air pressure with practically no effect from the movement of the aircraft. The center tube, however, is pointed in the direction of travel and is pressurized by the total of the local static air pressure and air pressure coming from the movement of the aircraft (air velocity). The pressure transducer measures the difference in total and static pressure.

Using Bernoulli's equation, aircraft velocity (airspeed) with help of pitot tube can easily be measured:

$$p_t = \left(p_s + r\frac{v^2}{2} \right),$$

$$v^2 = \frac{2(p_t - p_s)}{r}.$$

Here r is the air density, v is the velocity, p_t is the total pressure, p_s is the static pressure. The main approach of constructing the pitot tube based sensor is incorporating two perpendicular located pitot tubes. One of which measures V_x and another V_z (Fig. 1). Where V_x and V_z are the components of total velocity vector V_0.

The following is the representation of the incidence angle calculation:

$$\alpha = \arctan\frac{V_x}{V_z}.$$

The second element of integrated system of incidence angle measurement is accelerometer, which measures vertical acceleration a_z of the aircraft. Vertical acceleration is directly proportional to the incidence angle. This relation is given by the following expression:

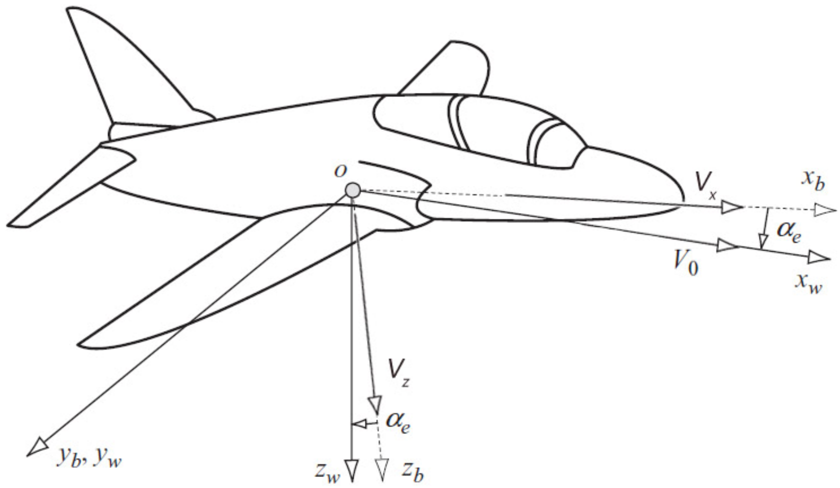

Fig. 1. Body ($ox_by_bz_b$) and wind ($ox_wy_wz_w$) reference systems

$$\frac{a_z}{g} = n\frac{\mathrm{L}}{\mathrm{W}} \approx \frac{\left(C_{L_0} + C_{L_\alpha}\alpha\right)\bar{q}\mathrm{S}}{W}. \qquad (1)$$

Here a_z is the vertical acceleration, L is the lift, W is the airplane weight, C_{L_0} is the lift coefficient (airplane) for zero incidence angle, $C_{L_\alpha} = \partial C_L / \partial\alpha$ is the variation of airplane lift coefficient with incidence angle, $\bar{q}$ is the airplane dynamic pressure.

Integrated system synthesis

Structure of the integrated system of an incidence angle measurement is shown in Fig. 2.

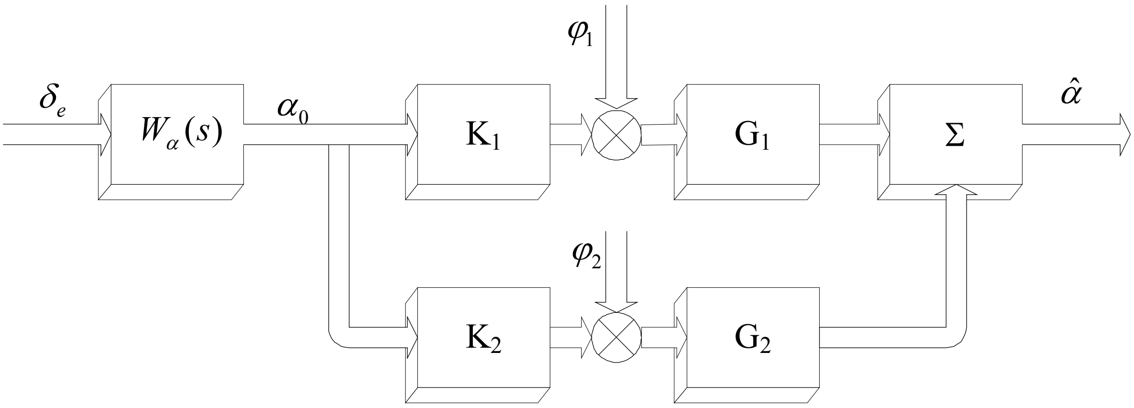

Fig. 2. Integrated system of incidence angle measurement

Here motion of an aircraft is characterizes by the matrix W and noise ψ [2]; K_1 is the transfer function of pitot tube system, φ_1 is the pitot tube system sensor noise, $S_{\varphi_1\varphi_1}$ is the power spectral density of pitot tube system noise, K_2 is the transfer function of accelerometer, φ_2 is the accelerometer sensor noise, $S_{\varphi_2\varphi_2}$ is the power spectral density of accelerometer sensor noise, r is the input signal (in given case incidence angle signal), S_{rr} is the power spectral density of input signal.

Power spectral density of the input signal r calculated as white noise, which "colored" by control object. Applying Weiner-Khinchine theorem, we obtain

$$S_{rr} = W(s) \times S_\delta \times W_*(s) = W(s) \times \frac{\sigma^2}{\pi} \times W(-s).$$

Here "*" designates Hermite conjugate, $S_\delta = \frac{\sigma^2}{\pi}$ is the power spectral density of a white noise; $W(s)$ is the transfer function of the aircraft, which after the short period approximation [3] can be represented as:

$$W(s) = \frac{1}{s^2 + 2\zeta\omega s + \omega^2}.$$

The power spectral densities of sensor noises φ_1 and φ_2 are determined as:

$$S_{\varphi_1\varphi_1} = K_1 \times S_\delta \times K_{1*} = \frac{\sigma_1^2}{\pi} \times K_1^2,$$

$$S_{\varphi_2\varphi_2} = K_2 \times S_\delta \times K_{2*} = \frac{\sigma_2^2}{\pi} \times K_2^2,$$

where K_2 can be represented as:

$$K_2 = \frac{1}{s^2 + 2\zeta_2\omega_2 s + \omega_2^2}.$$

Let us introduce new variables defined as follows:

$$K_0 = \begin{bmatrix} K_1 \\ K_2 \end{bmatrix},\ \varphi_0 = \begin{bmatrix} \varphi_1 \\ \varphi_2 \end{bmatrix},$$

$$G_0 = (G_1, G_2),\ \rho_0 = K_0 r = \begin{bmatrix} K_1 r \\ K_2 r \end{bmatrix}$$

The power spectral densities of ρ_0 and φ_0 (assuming, that signals φ_1 and φ_2 are not correlated and cross spectral densities are zeros) defined as:

$$S'_{\rho_0\rho_0} = \begin{bmatrix} S'_{rr}K_1^2 & K_1 S'_{rr} K_2 \\ K_2 S'_{rr} K_1 & S'_{rr} K_2^2 \end{bmatrix},\ S'_{\varphi_0\varphi_0} = \begin{bmatrix} S'_{\varphi_1\varphi_1} & S'_{\varphi_2\varphi_1} \\ S'_{\varphi_1\varphi_2} & S'_{\varphi_2\varphi_2} \end{bmatrix} = \begin{bmatrix} S'_{\varphi_1\varphi_1} & 0 \\ 0 & S'_{\varphi_2\varphi_2} \end{bmatrix}. \quad (2)$$

We calculate matrix $D_0 D_{0*}$ as follows:

$$D_0 D_{0*} = S'_{\rho_0\rho_0} + S'_{\varphi_0\varphi_0} = \begin{pmatrix} a & b \\ c & d \end{pmatrix}, \quad (3)$$

where

$$a = K_1\delta_1^2 + \frac{K_1^2\delta^2}{(s^2 + 2\zeta\omega s + \omega^2)(s^2 - 2\zeta\omega s + \omega^2)},$$

$$b = \frac{K_1\delta^2}{(s^2 + 2\zeta\omega s + \omega^2)(s^2 - 2\zeta\omega s + \omega^2)(s^2 + 2\zeta_2\omega_2 s + \omega^2)},$$

$$c = \frac{K_1\delta^2}{(s^2 + 2\zeta\omega s + \omega^2)(s^2 - 2\zeta s + \omega^2)(s^2 + 2\zeta_2\omega_2 s + \omega^2)},$$

$$d = \frac{\delta^2}{(s^2 + 2\zeta\omega s + \omega^2)(s^2 - 2\zeta\omega s + \omega^2)\left|(s^2 + 2\zeta_2\omega_2 s + \omega^2)\right|^2} +$$

$$+ \frac{\delta_2^2}{(s^2 + 2\zeta_2\omega_2 s + \omega^2)(s^2 - 2\zeta_2\omega_2 s + \omega^2)}.$$

Factorization of the matrix (3) by the Davis method combine with method of undetermined coefficients results in the following expression:

$$D_0 \approx \frac{\sigma}{\sqrt{\pi}}\frac{\gamma_1}{\sqrt{2}}\begin{pmatrix} a_1 & b_1 \\ c_1 & d_1 \end{pmatrix}, \tag{4}$$

where

$$a_1 = -K_1,$$

$$b_1 = \frac{K_1\left(s + 0.5\sqrt{-4\omega^2 + \zeta^2\omega^2 - 2\sqrt{-\frac{8}{\gamma_1^2} + 16\omega^4\xi^4}}\right)\left(s + 0.5\sqrt{-4\omega^2 + \zeta^2\omega^2 + 2\sqrt{-\frac{8}{\gamma_1^2} + 16\omega^4\xi^4}}\right)}{(s^2 + 2\zeta\omega s + \omega^2)}$$

$$c_1 = \frac{1}{(s^2 + 2\zeta_2\omega_2 s + \omega_2^2)},$$

$$d_1 = \frac{\left(s + 0.5\sqrt{-4\omega^2 + \zeta^2\omega^2 - 2\sqrt{-\frac{8}{\gamma_1^2} + 16\omega^4\xi^4}}\right)\left(s + 0.5\sqrt{-4\omega^2 + \zeta^2\omega^2 + 2\sqrt{-\frac{8}{\gamma_1^2} + 16\omega^4\xi^4}}\right)}{(s^2 + 2\zeta\omega s + \omega^2)(s^2 + 2\zeta_2\omega_2 s + \omega_2^2)}$$

During factorization was designation as follows:

$$\gamma_1 = \frac{\sigma_1}{\sigma},\ \gamma_2 = \frac{\sigma_2}{\sigma}.$$

And taking into consideration that $\sigma << \sigma_1$ and $\sigma << \sigma_2$ we can assume that $\gamma_1 \approx \gamma_2$. Considering that

$$\Phi_0 = \begin{pmatrix} K_1^{-1} & 0 \end{pmatrix},$$

and substituting (2) and (4) into the following equation

$$T = T_0 + T_+ + T_- = \Gamma_*^{-1} M_* P_*^{-1} R \Phi_0 S'_{\rho_0\rho_0} D_{0*}^{-1}, \tag{5}$$

after execution operation of separation of matrix (5) we can calculate the filter matrix G_0 by the formula [3]:

$$G_0 = \Gamma^{-1}(T_0 + T_+)D_0^{-1}.$$

For the real plant with transfer function

$$W(s) = \frac{1}{s^2 + 1.988s + 8.0656},$$

and for the accelerometer given by (1) we use numerical values

$$\zeta_2 \approx 0.707,\ \omega_2 = 1000Hz.$$

finally the matrix of filter G_0 will be

$$G_0 = \frac{\pi}{\sigma^2}\begin{pmatrix} a_2 & b_2 \end{pmatrix},$$

where

$$a_2 = \frac{186.601s + 35189.9}{K_1(s^2 + 375.19s + 70388)},$$

$$b_2 = \frac{0.186601s^3 + 299.043s^2 + 236.359s + 3.51899 \cdot 10^5}{(s^3 + 375.19s^2 + 70388s + 0.070388)}.$$

To verify performance of the estimator, which was obtained using linear model, in real conditions, we conduct numerical simulations. The results of simulation are represented in Fig. 3, Fig. 4.

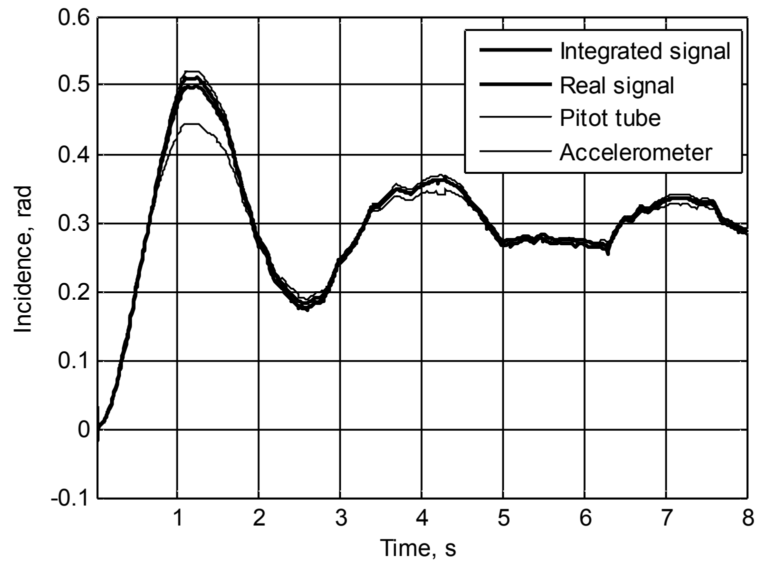

Fig. 3. Result of simulation (general system)

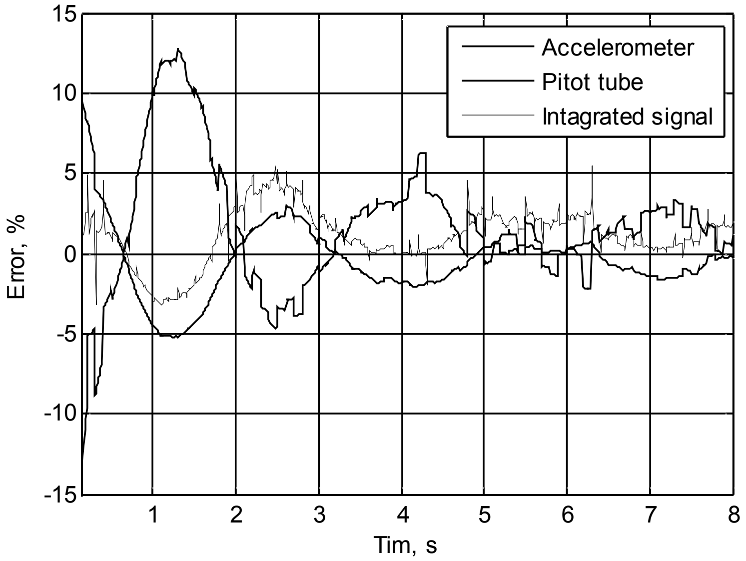

Fig. 4. Relative error (general system)

From graphs in Fig. 3 and 4 one can see that incidence angle measurement is significantly improved by means of signal integration.

Simplified integrated system

Let us consider simplified model of accelerometer and find the matrix G using the same algorithm, described above.

Power spectral densities of sensor noises φ_1 and φ_2 are determined as

$$S_{\varphi_1\varphi_1} = K_1 \times S_\delta \times K_{1*} = \frac{\sigma^2}{\pi} \times K_1^2,$$

$$S_{\varphi_2\varphi_2} = K_2 \times S_\delta \times K_{2*} = \frac{\sigma^2}{\pi} \times K_2^2.$$

Matrix $D_0 D_{0*}$ is then calculated as follows:

$$D_0 D_{0*} = S'_{\rho_0\rho_0} + S'_{\varphi_0\varphi_0} = \frac{\sigma^2}{\pi}\begin{bmatrix} K_1^2\left(1+|W|^2\right) & K_1K_2|W|^2 \\ K_1K_2|W|^2 & K_2^2\left(1+|W|^2\right)\end{bmatrix} =$$

$$= \frac{\sigma^2}{\pi}\begin{bmatrix} K_1^2\left(1+\left|\frac{1}{(s^2+2\zeta\omega s+\omega^2)}\right|^2\right) & K_1K_2\left|\frac{1}{(s^2+2\zeta\omega s+\omega^2)}\right|^2 \\ K_1K_2\left|\frac{1}{(s^2+2\zeta\omega s+\omega^2)}\right|^2 & K_2^2\left(1+\left|\frac{1}{(s^2+2\zeta\omega s+\omega^2)}\right|^2\right)\end{bmatrix}. \quad (6)$$

After factorization of the matrix (6) by the Davis method results in

$$D_0 \approx \frac{\sigma}{\sqrt{\pi}} \frac{\gamma_1}{\sqrt{2}} \begin{pmatrix} a_3 & b_3 \\ c_3 & d_3 \end{pmatrix},$$

Where

$$a_3 = -K_1,$$

$$b_3 = \frac{K_1 \left(s + 0.5\sqrt{-4\omega^2 + \zeta^2\omega^2 - 2\sqrt{-\frac{8}{\gamma_1^2} + 16\omega^4\xi^4}} \right)\left(s + 0.5\sqrt{-4\omega^2 + \zeta^2\omega^2 + 2\sqrt{-\frac{8}{\gamma_1^2} + 16\omega^4\xi^4}} \right)}{(s^2 + 2\zeta\omega s + \omega^2)},$$

$$c_3 = K_2,$$

$$d_1 = \frac{\left(s + 0.5\sqrt{-4\omega^2 + \zeta^2\omega^2 - 2\sqrt{-\frac{8}{\gamma_1^2} + 16\omega^4\xi^4}} \right)\left(s + 0.5\sqrt{-4\omega^2 + \zeta^2\omega^2 + 2\sqrt{-\frac{8}{\gamma_1^2} + 16\omega^4\xi^4}} \right)}{(s^2 + 2\zeta\omega s + \omega^2)(s^2 + 2\zeta_2\omega_2 s + \omega_2^2)}$$

.

Matrix of filter G_0 will be following:

$$G_0 = \frac{\pi}{\sigma^2}\begin{pmatrix} a_4 & b_4 \end{pmatrix}.$$

Here

$$a_4 = \frac{186.601\text{s} + 35189.9}{K_1\left(s^2 + 375.19\text{s} + 70388\right)},$$

$$b_4 = \frac{186.601\text{s} + 35189.9}{K_2\left(s^2 + 375.19\text{s} + 70388\right)}.$$

The results of the corresponding numerical simulation are represented as graphs shown in Fig. 5 and 6.

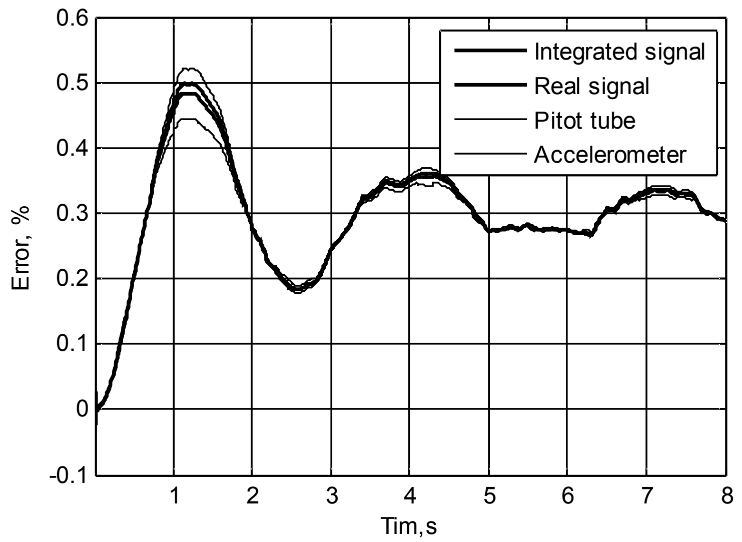

Fig. 5. Result of simulation (simplified system)

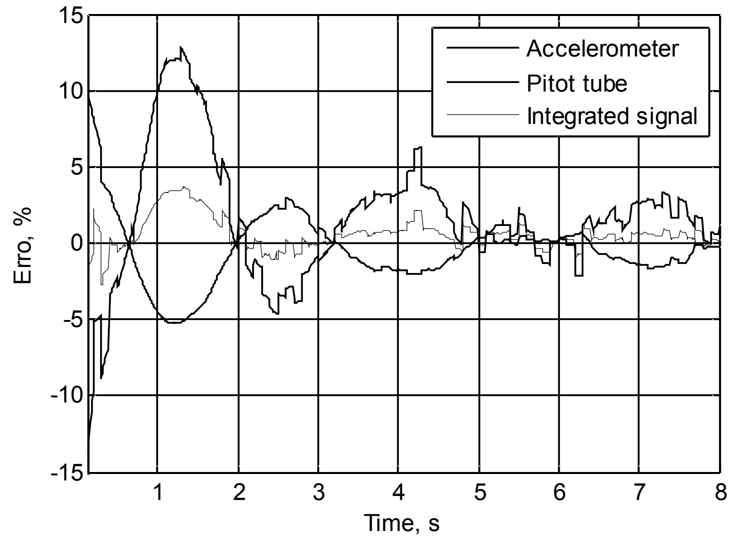

Fig. 6. Relative error (simplified system)

Comparison of systems performances

Let us compare performance of the general and simplified integrated systems. The relative errors of these systems are shown in Fig. 7.

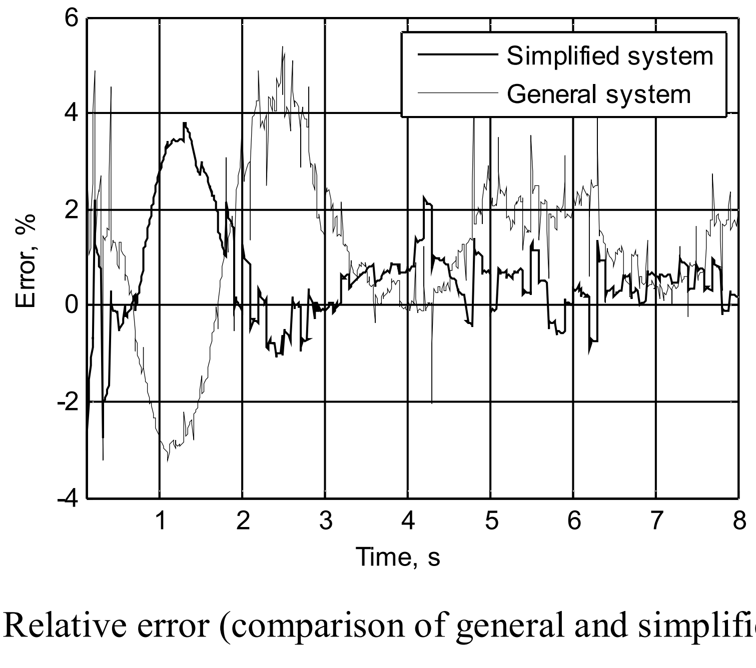

Fig. 7. Relative error (comparison of general and simplified systems)

Here one can see, that simplified system still delivers performance comparable with more complicated design.

Conclusions

Presented above synthesis of the stationary multidimensional filter resulted in integrated system capable of improved incidence angle measurement by means of combining pitot tube sensors system output with the output of the normal accelerometer. Excellent performance of the developed systems is demonstrated by numerical simulations in real world conditions.

The further analysis of the application of Kalman Filtering to synthesis integrated system for incidence angle measurement is viewed as a possible future development of the current research.

References

1. *Titterton D.H., Weston J.L.* Strapdown Inertial Navigation Technology // AIAA, 2004. – 580 p.
2. *Apostolyuk V.A., Boiko V.M.* Integrated System of Incidence Angle Measurement // Proceedings of AVIA-2011, Vol. 3.– pp. 9.31-9.34.
3. *Блохін Л.М., Буриченко М.Ю.* Статистична динаміка систем управління // Київ: НАУ, 2003. – 208 p.
4. *Michael V.Cook* Flight Dynamics Principles //Elsevier Linacre House, 2007. – 468 p.
5. *Roskam, J* Airplane Flight Dynamics and Automatic Flight Controls // DARcorporation, 1995. – 576 p.